Stability of bubbly liquids and its connection to the process of cavitation inception

D. Fuster, K. Pham, and S. Zaleski

Citation: Physics of Fluids (1994-present) **26**, 042002 (2014); doi: 10.1063/1.4870820
View online: http://dx.doi.org/10.1063/1.4870820
View Table of Contents: http://scitation.aip.org/content/aip/journal/pof2/26/4?ver=pdfcov
Published by the AIP Publishing

PHYSICS OF FLUIDS **26**, 042002 (2014)

Stability of bubbly liquids and its connection to the process of cavitation inception

D. Fuster,[1,a)] K. Pham,[2] and S. Zaleski[3]
[1]*CNRS, UMR 7190, Institut Jean Le Rond d'Alembert, F-75005 Paris, France*
[2]*Unité de Mécanique, École Nationale Supérieure de Techniques Avancés, 91761 Palaiseau, France*
[3]*UPMC Univ Paris 06, UMR 7190, Institut Jean Le Rond d'Alembert, F-75005 Paris, France*

(Received 24 November 2013; accepted 20 March 2014; published online 14 April 2014)

This paper presents a potential energy approach for the investigation of the stability of bubbly liquids. Using the system's free energy variations with respect to the void fraction as a stability criterion for the whole system, we consider that sudden bubble expansion occurs only when the bubble cluster expansion is energetically favorable. The results obtained provide new insight into the behavior of pre-nucleated liquids when the inception point is reached as well as a simple method to estimate the energy exchanges between a bubble cluster and its environment when the kinetic energy is negligible compared to the elastic energy stored during tension and compression processes. In addition to the radius of the initial nuclei, the concentration and polydispersity are shown to exert an important influence on the response of the system after inception. © *2014 AIP Publishing LLC*. [http://dx.doi.org/10.1063/1.4870820]

I. INTRODUCTION

The stability of bubbly liquids finds interest in various applications related to the phenomenon of bubble inception. In general, the cavitation inception point is defined in terms of the cavitation number. Below a certain critical value, a sudden vaporization of the liquid and subsequent bubble growth is observed. Blander and Katz[1] made a complete review of classical theories and more recently, Uline and Corti[2] and Shen and Debenedetti[3] have proposed new theories. Theories based on statistical mechanical approaches describe the process of nucleation at the molecular level, predicting the nucleation rate at given conditions.

To experimentally reach the homogeneous nucleation limit in standard liquids is extremely difficult.[4,5] In practical applications with standard fluids, such as water, bubble nuclei already present in the system lead to the sudden appearance of bubbles once the inception point is reached. Thus, it is commonly accepted that this process is controlled by the bubble nuclei initially present in the system. Recent experimental techniques have shown that even in degasified liquids, small bubble nuclei, called surface nanobubbles, remain in the system, tending to stick to the solid's surface.[6] The size of these bubble nuclei can vary from the order of nanometers to tenths of micrometers, depending on the degree of degasification of the liquid. Remarkably, these nanobubbles can persist in the liquid for days,[7] which contradicts the quick dissolution rates that one may expect from the pressure gradient generated at the interface as a consequence of the Laplace term.

The effect of the bubble nuclei in practical applications is clearly shown by Keller,[8] who compares the critical cavitation number for tap, degassed, and filtered tap water. When nuclei are extremely small, the system is stable to very large negative pressures.[9] This process is analogous to the large temperatures locally reached during the process of bubble nucleation in boiling.[10] Various parameters that influence the concentration and characteristics of these nuclei are also known to play an important role in the process.[11] Acosta and Parkin,[12] Rood,[13] and Brennen[14] present reviews about

a)Electronic mail: fuster@dalembert.upmc.fr

the various mechanisms influencing the critical inception point. Atchley and Prosperetti[15] present a model to capture the influence of the main parameters on the process of bubble nucleation. These studies stress the importance of additives, liquid properties, and surface smoothness. Finally, the gas content (e.g., the initial volume fraction of bubbles) also plays an important role in the process of nucleation and the posterior dynamic response of the system. Above a certain concentration, the injection of air reduces the intensity of the shock waves generated by the bubble collapse in hydrofoils.[16,17] More recently, Ida *et al.*[18] have investigated the influence of microbubbles on the damage induced by pressure waves.

The stability of a single bubble is typically investigated using the linearized version of the Rayleigh-Plesset equation.[19,20] If the mass of gas does not change significantly during the characteristic time of the tension process, the bubble is unstable for pressures below a certain critical pressure. The bubble radius in equilibrium with this critical pressure is known as Blake's radius.[19] This analysis is taken as reference for most engineering applications given that the investigation of more general situations involving multiple bubbles is difficult. For instance, there are few theoretical works in the literature dealing with the effect of the initial content of air in the system (problem numerically studied by Ida *et al.*[21]) on the process of bubble inception.

In this paper, we use classical thermodynamic concepts to investigate the stability of pre-nucleated liquids. The derivative of the system's Helmholtz free energy with respect to the void fraction is shown to provide a criterion that can be used to derive the stability regions of liquids under tension. This analysis allows us to define a clear criterion for the "bubble inception conditions" that we define as the conditions in which bubble expansion is energetically favored. A similar concept is indeed used in the crevice model[15] to investigate the stability of bubbles attaching to walls. This paper exploits this property to gain new insight into the stability of multibubble systems and to investigate the impact of two parameters not considered in previous studies on the process of bubble inception: the effect of the initial gas content and polydispersity. The approach proposed in this paper can also be used for the prediction of the evolution of the void fraction and system's pressure in cavitating flows, thus allowing to estimate the energy exchanges produced between the bubble cloud and its environment. The simplicity of the method should serve to characterize complex systems containing several bubbles where more complete analyses taking into account dynamic effects become cumbersome and the results difficult to interpret.

II. STABILITY ANALYSIS

This paper discusses the stability of different bubbly liquid flows using the concept of the system's potential energy ψ. Provided a state given by a set of independent variables $\boldsymbol{x}$, we determine how the system evolves when we introduce a small perturbation in the void fraction, β, which is also translated into a perturbation in the bubble volume. According to classical thermodynamics, when $\frac{\partial \psi}{\partial \beta} \geq 0$, the system tends to minimize the energy by reducing the volume, that is, compressing the bubbles. Otherwise bubbles expand without any extra source of external energy in order to reduce the total system's energy and a sudden bubble expansion and liquid evaporation occurs. Thus, we define as "bubble inception conditions" the set of x equilibrium points ($\frac{\partial \psi}{\partial \beta} = 0$) for which $\frac{\partial^2 \psi}{\partial \beta^2} < 0$.

The investigation of the general problem is too involved. For that reason, in this work we restrict ourselves to systems under tension with spherical nuclei whose mass of insoluble gas remains constant along the process. The choice of the system's potential depends on the situation considered. For instance, the Gibbs free energy is typically used to investigate the stability of systems at a fixed pressure and temperature, whereas the Helmholtz free energy F is used for processes at constant temperature and volume. In a bubble cloud, we expect the effective pressure *felt* can be influenced not only by the external pressure disturbance, but also by the surrounding bubbles. In other situations, such as a bubble inside a cavity whose volume can be modified, the bubble can influence the pressure of the entire system. Assuming that pressure variations are externally induced in the system with a frequency ω much smaller than the bubble natural frequency ω_b, any influence of either the surrounding bubbles or of the domain boundaries is relevant for nondimensional distances smaller than 1, $\frac{\omega L}{c} < 1$, where c is the speed of sound and L represents either the characteristic inter-bubble

distance or the distance to a domain boundary. Thus, in systems for which the characteristic length is smaller than the critical length $L_c = c/\omega$ the Helmholtz free energy turns out to be the suitable potential.

We consider situations where we decrease the system's pressure until reaching inception. When the critical point is reached, pressure quickly recovers to a new equilibrium value, which typically is around the liquid vapor pressure. The choice of the Helmholtz free energy is made consistent with the assumption that the process is isothermal. This assumption is justified for states before inception, where the bubble temperature variations do not have an appreciable impact on the system's temperature.[15] After inception occurs, this hypothesis may be questionable since the temperature variations mostly inside the bubbles are expected to be important. In any case, one must keep in mind that the free energy is defined for the entire system and therefore, while the averaged system's temperature variations are small, this assumption is still representative of the overall system's response. Thus, the Helmholtz free energy is expected to be a suitable potential not only before inception, but also during the first moments after inception when the void fraction still remains relatively low. For very large void fractions, thermal effects and also mass transfer effects may be relevant and further extensions of the current approach would be required.

The Helmholtz's free energy variations can be obtained from the integration along reversible paths from a reference equilibrium state at constant pressure p_0 as

$$\Delta F = -\int_0^{V-V_0} p' dV,$$

where V_0 is the volume of the bubbly liquid system initially in equilibrium and p' represents the perturbed state of the system with respect to its equilibrium state, such that $p' = p - p_0$. This definition is important in order to ensure that the reference state of the bubbly liquid at p_0 is in equilibrium with its environment before applying any external force on it.

Pressure and volume are linked through the state equation. For single phase flows, the state equation is usually simple if we assume some idealized behavior (ideal gas, incompressible liquid, etc.). For mixtures, one possibility is to compute the energies involved in each phase separately, where the state equation and density and pressure variations are linked through the definition of the speed of sound. For a system with N_b bubbles, the total volume can be computed as the sum of the liquid volume, V_l and the sum of all individual bubble volumes, $V_{b,i}$. Following Fuster and Colonius,[22] we choose as a representative pressure for the system the liquid pressure. Thus,

$$\Delta F = -\int p_l' dV_l - \sum_{i=1}^{N_b} \int p_l' dV_{b,i}.$$

For a control volume with a given mass of liquid M_l, we can relate volume and pressure variations through the definition of the speed of sound $dp_l = c_l^2 d\rho_l$, where $\rho_l = M_l/V_l$ is the liquid density. Analogously, we use the ideal gas model for the bubble interior to relate the mass of immiscible gas $M_b = \sum_{i=1}^{N_b} M_{b,i}$ and volume variations with the pressure variations inside the bubbles $p_{b,i}$,

$$\Delta F = \int_0^{p_l - p_0} \frac{p_l' M_l}{\rho_l^2 c_l^2} dp_l' + \sum_{i=1}^{N_b} \int_0^{p_l - p_0} \frac{p_l' M_{b,i}}{p_{b,i}\rho_{b,i}} dp_{b,i},$$

where we have neglected mass transfer effects between the two phases as a first approximation. Because we place ourselves in the case of slow perturbations, the system and the bubble pressure have time to reach mechanical equilibrium and the sequence of possible equilibrium states given by Laplace's equation. For every individual bubble present in the system, we write

$$p_l = p_{b,i} - \frac{2\sigma}{R_i}, \tag{1}$$

where σ is the surface tension and R_i is the radius of the ith bubble. We remark that in addition to not considering mass transfer effects, we have also neglected the viscous stresses at the interface, which for small bubbles implies that $p_l \gg \mu_l \dot{R}/R_i$, where μ_l is the liquid viscosity. Writing the characteristic bubble interface velocity as a function of the forcing frequency, f, and the bubble

oscillation amplitude ΔR, $\dot{R} \approx \Delta R f$, the analysis presented here is restricted to situations where $f \ll p_l R_0/(\Delta R \mu_l)$, which is expected to be valid due to the small bubble radius variations before inception occurs. Assuming that the mass of gas and the number of bubbles remains constant along the process, the bubble pressure can be expressed as a function of the bubble radius as

$$p_{b,i} = p_{g,i0}\left(\frac{R_{i0}}{R_i}\right)^{3\kappa}, \tag{2}$$

where $p_{g,i0}$ is the partial pressure of the insoluble gas contained in the *ith* bubble in equilibrium with the surrounding medium at p_0 and T_0 and κ is the effective polytropic coefficient.

Using Eqs. (1) and (2) it is possible to relate bubble pressure variations and bubble radius variations

$$dp_{b,i} = -3\kappa \frac{p_{b,i}}{R_i} dR_i$$

such that

$$\begin{aligned}\Delta F = & \int_0^{p_l - p_0} \frac{p_l' M_l}{\rho_l^2 c_l^2} dp_l' \\ & - \sum_{i=1}^{N_b} \int_{R_{0i}}^{R_i} \kappa p_{g,i0} \left(\frac{R_{0i}}{R_i}\right)^{3\kappa} 4\pi R_i^2 dR_i \\ & + \sum_{i=1}^{N_b} \int_{R_{0i}}^{R_i} 8\kappa\sigma\pi R_i dR_i. \end{aligned} \tag{3}$$

The number of bubbles present in the system can be obtained from the void fraction definition

$$\beta = \frac{4}{3}\pi n \overline{R^3}, \tag{4}$$

where n represents the number of bubbles per unit volume. The equation above defines the void fraction of the system in terms of the averaged radius which is usually obtained as $\overline{R^3} = \int_0^\infty \hat{R}^3 f(\hat{R}) d\hat{R}$ where $f(\hat{R})$ is assumed to be known.

The system formed by Eqs. (1), (3) and (4) can be solved to obtain the evolution of the system potential as a function of the void fraction for a constant mass of immiscible gas. In Secs. II A and II B, we considered some simplified situations in order to gain more insight about the influence of different parameters characterizing the initial population of bubble nuclei.

A. Monodisperse bubble nuclei distributions

Let us consider a monodisperse bubble cluster in initial equilibrium made of bubble nuclei with radius R_0 and initial concentration of bubble nuclei β_0, both parameters defined at the reference pressure p_0 and temperature T_0. Taking a system of volume V with N bubbles of the same radius R, the Helmholtz free energy takes the form

$$\Delta F = \frac{1}{2}\frac{(p_l - p_0)^2}{\rho_l c_l^2}(1-\beta)V - 3p_{g,0}\ln\left(\frac{R}{R_0}\right)\beta V + 3\frac{\sigma}{R}\beta V, \tag{5}$$

where we have imposed that the bubble response is isothermal ($\kappa = 1$). This expression contains the different energies present in the system, namely, the elastic energy stored in the liquid phase, the elastic energy in the gas, and the surface energy stored at the interface. In Secs. II A 1 and II A 2, we discuss the stability of the system as a function of the concentration of gas in the system.

1. The dilute limit

When the void fraction is low enough ($\beta \to 0$) the Helmholtz free energy of the system simplifies to

$$\Delta F = \frac{1}{2} M_l \frac{(p_l - p_0)^2}{\rho_l^2 c_l^2}.$$

This expression for the elastic energy stored in the liquid is similar to that found by Landau and Lifshitz[23] for acoustic waves propagating in slightly compressible liquids and it reveals an important feature of dilute bubbly liquids under tension: the system's energy is mostly stored in the liquid as an elastic energy due to the liquid compressibility.

The equilibrium points of the system can be obtained setting to zero the first derivative of the potential with respect to the void fraction,

$$\frac{\partial F}{\partial \beta} = M_l \frac{p_l - p_0}{\rho_l^2 c_l^2} \frac{\partial p_l}{\partial \beta} = 0,$$

which defines three equilibrium points: one found at $p = p_0$ and other two obtained by imposing $\frac{\partial p_l}{\partial \beta} = 0$. For a monodisperse bubble cluster, we readily find that

$$\frac{\partial p_l}{\partial \beta} = \frac{\partial p_l}{\partial R} \frac{\partial R}{\partial \beta} = \frac{1}{4\pi n R^2} \left(\frac{3 p_{g,0}}{R} - \frac{2\sigma}{R^2} \right) = 0.$$

Thus, the two additional equilibrium points are found to be Blake's radius and $R = \infty$. The stability of these points is discussed as a function of the sign of the second derivative. Consistent with the classical stability analysis from the Rayleigh-Plesset equation, Blake's radius is unstable (see Figure 1) whereas the point at $R = \infty$ is stable.

The discussion above proves that we can understand the Blake radius as a critical radius beyond which the system enters an unstable state in which bubbles expand and the system's pressure tends to recover the vapor pressure. Otherwise the system tends to recover its initial equilibrium position. This process resembles brittle fracture in solid mechanics, where the presence of initial micro-cracks induces the fracture of solids at small deformations. In the case of liquids, the relative deformation of the control volume ϵ can be directly attributed to the volume change induced by the bubble nuclei present in it. In reduced form, we can express this deformation as

$$\epsilon = \frac{\beta - \beta_0}{\beta_c - \beta_0}, \tag{6}$$

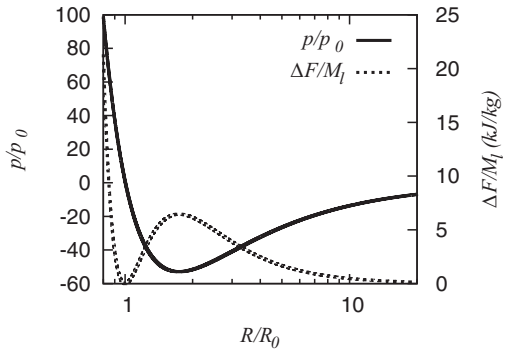

FIG. 1. Nondimensional pressure and bubble cluster's elastic potential as a function of the nondimensional bubble radius for a monodisperse bubble cluster.

where β is the void fraction at every instant, β_0 is the void fraction in the reference state, and β_c is the critical void fraction obtained using Blake's radius, R_c, which can be explicitly expressed as

$$\frac{R_c}{R_0} = \sqrt{3\left(1 + \frac{p_0 R_0}{2\sigma}\right)}. \tag{7}$$

This deformation is $\epsilon = 1$ at the inception point and it grows monotonically with R/R_0 for the monodisperse case. The convenience of the definition of this new variable will become clearer when discussing the effect of polydispersity.

2. Stability of bubble clusters at large void fractions

In Blake's analysis, the only parameter related to the properties of the bubble nuclei initially present in the system is the bubble radius. However, it is desirable to study the influence of other global parameters. One of the advantages of the current approach with respect to the analysis of the single bubble case is that it can be also used to theoretically investigate the influence of parameters related to the initial population of bubble nuclei on the stability of the system, such as the initial air concentration β_0. This finds interest in various applications. For instance, it is well known that the injection of air above a certain threshold value reduces the intensity of the shock waves, and thus the intensity of noise, generated during the process of bubble inception and later collapse in hydrofoils.[16,17]

From Eq. (5) it is easy to verify that the energy stored at the interface tends to stabilize the system. In the low concentration limit, when the critical void fraction β_c is reached, the elastic energy released by the liquid provides the energy required by the interface to make bubbles grow without any source of external energy. However, the amount of interface elastic energy required is proportional to the amount of gas present in the system and therefore, there exists a critical gas void fraction for which the elastic energy released by the liquid is not compensated by the increase of elastic surface energy required at the interface. This effect can be clearly seen in Figure 2, where we represent the evolution of the Helmholtz free energy for different initial concentrations of air. When increasing the amount of air and for extremely low concentrations, we expect the number of bubble nuclei present in the system to increase and therefore, the number of noise emitters. After a critical initial air concentration is reached, the system becomes stable in the sense that the bubble expansion is no longer energetically favored. Thus, while the number of bubble nuclei increases, the importance of dynamic effects is attenuated for given operational conditions. The critical concentration value obtained is relatively low and therefore the isothermal assumption still holds as the bubbles are not expected to have an impact on the averaged system's temperature. It is remarkable that the air concentration threshold for which air starts damping the noise emitted is consistent with the strong noise reduction experimentally observed by Reisman *et al.*,[16,17] where the injection of very low amounts of air is shown to significantly damp the noise generated during the bubble inception.

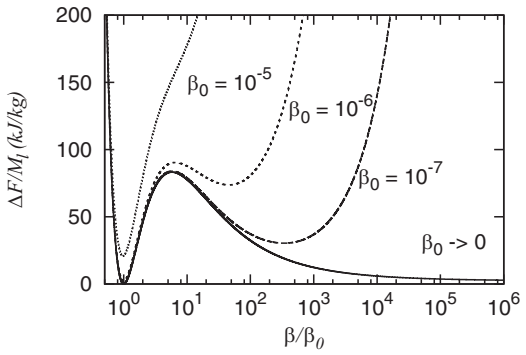

FIG. 2. Helmholtz free energy of a monodisperse bubble cluster made of bubble nuclei of $R_0 = 0.1$ μm versus void fraction for four different initial concentration of air bubbles: $\beta_0 = 0, 10^{-7}, 10^{-6}, 10^{-5}$.

An estimation of the initial bubble concentration required to stabilize the process of bubble inception can be obtained as follows. Because the elastic energy stored in the gas phase is usually negligible, the critical void fraction (β_c) is given by the balance of the tension energy and the energy stored at the surface. For small bubble nuclei where the absolute value of the critical tension is larger than the reference pressure, the surface tension term becomes more important than the maximum elastic energy stored in the liquid phase during the tension stage for initial void fractions larger than a critical void fraction β_0^*

$$\beta_0 > \beta_0^* = \frac{0.171}{\sqrt{1+\frac{p_0 R_0}{2\sigma}}}\frac{\sigma}{R_0 \rho_l c_l^2}.$$

B. Polydisperse bubble nuclei distributions

Section II A has derived expressions for the monodisperse case. However, in practical applications the bubble distribution is polydisperse. When the bubbles initially present in the system have different sizes, p_l must verify the Laplace equation (1) of every bubble in the system. Thus, the system's pressure is indeed governed by the largest bubble in the system given that it imposes the most stringent condition at a given void fraction. To illustrate this mechanism, Figure 3 represents the evolution of a system with a discrete bubble nuclei distribution of 0.5, 1, 2, and 4 nm, respectively. When starting decreasing the system's pressure, all bubbles expand (state 1), the minimum achievable pressure being the critical pressure of the largest bubble (state 2). From this point on, it is no longer possible to decrease the system's pressure in an infinitely slow experiment given that the largest bubble tends to expand and to make the system's pressure recover (states 3 and 4). When the largest bubble starts expanding, the surrounding bubbles tend to contract given that they have not reached their corresponding Blake's radius. This phenomenon makes possible the appearance of multiple equilibrium pressures for void fractions lying inside a specific range. Note that this situation is different from the monodisperse case, where void fraction and bubble radius are always proportional. In the polydisperse case, the volume increase of the largest bubble may not compensate the volume compression of the rest of bubbles considered in the system.

To obtain the correct evolution of the system's pressure as the void fraction varies, one needs to solve for the complete set of Laplace's equations applied to every single bubble plus the equation defining the global void fraction. For systems with a known bubble radius distribution, it is possible to solve for this system of equations as follows. We discretize the bubble radius distribution in N subintervals. Then we increase progressively the radius of the largest bubble present in the system

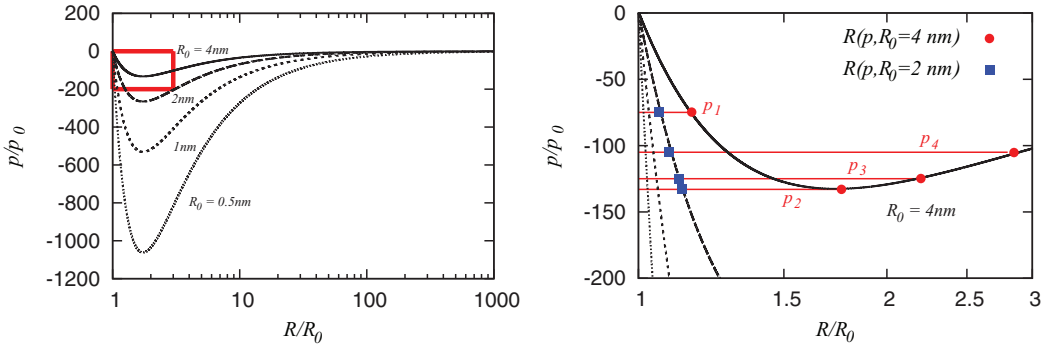

FIG. 3. Left: Nondimensional pressure versus the nondimensional bubble radius for different initial bubble sizes. Right: Zoomed view. For reference, we show a sequence of mechanical equilibrium states (from 1 to 4) and the corresponding equilibrium pressure and bubble radius for the largest bubble present in the system ($R_0 = 4$ nm with dots) and for a 2 nm bubble (squares). In a system with bubbles of different sizes, all bubbles expand when the system's pressure start decreasing (state 1). At the largest bubble Blake's radius, the pressure pass through a minimum (state 2). After this point, the pressure of the system recovers as the largest bubble expands (states 3 and 4). As the Blake's radius for small bubbles is not reached, these bubbles compress when the system's pressure recovers (states 3 and 4).

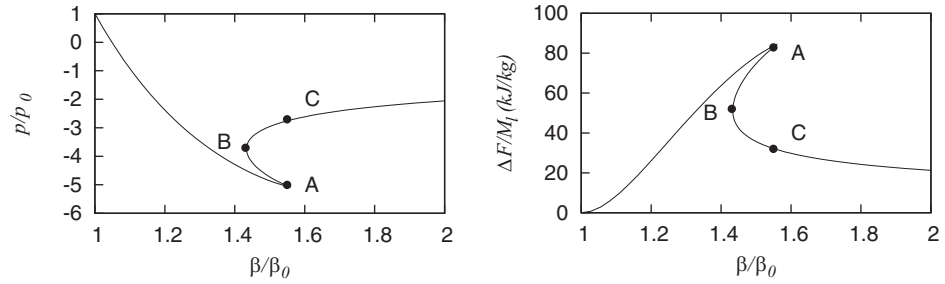

FIG. 4. Pressure (left) and Helmholtz free energy (right) of a polydisperse system versus void fraction. The system reaches a point at maximum tension (A) after which the volume of the system decreases still in a stable configuration until $\frac{\partial F}{\partial \beta} < 0$ (point B). In systems where the volume variations are imposed, the system equilibrium position changes from point A to point C instantaneously, becoming unstable. The initial bubble distribution obeys a lognormal size distribution with $\sigma = 0.7$ and $R_0^{ref} = 10$ nm. The maximum radius is set to $R_0^{max} = 100$ nm.

$R_{\max}$. The Laplace equation is assumed to hold for every bubble, and in particular for the largest bubble, therefore, for a given $R_{\max}$ we work out the corresponding equilibrium pressure using the Laplace equation (1). Once the pressure is obtained we solve for the bubble radius of the rest of bubbles present in the system using the Laplace equation applied to each bubble. Note from Figure 3 that for a given pressure the Laplace equation may have two possible equilibrium radius as solution. Thus, an iteration procedure is used where we use as an initial guess the radius from the previous equilibrium state. Finally, the void fraction in the system is computed applying Eq. (4). This procedure allows us to obtain $p(\beta)$, which can be taken as a prediction of the evolution of the system's pressure as a function of bubble concentration, and also the evolution of the system's potential energy. As it is often the case in physics, potential energy arguments may predict the evolution of real systems in some cases, but of course not in all of them. In real systems, potential energy is exchanged with kinetic energy making the analysis significantly more complex. The comparison between the system's potential solution and the response of more elaborated models including dynamic effects and also experimental data should clarify which effects and in which conditions the phenomena captured by simple potential analyses can help to interpret the response of complex systems.

As an example, we consider the response of a system with an initial bubble distribution obeying the following law:

$$f(R_0^*) = \begin{cases} \frac{1}{aR_0^* Q \exp\left(-\frac{\ln^2 R_0^*}{2a^2}\right)} & R_0^* \le R_0^{max}/R_0^{ref} \\ 0 & R_0^* > R_0^{max}/R_0^{ref} \end{cases},$$

where $R_0^* = R_0/R_0^{ref}$, being R_0^{ref} the averaged radius, R_0^{max} is the maximum radius present in the liquid, a is a measure of the dispersion of the bubble distribution, and Q is a correction factor introduced to satisfy that the integral of the probability distribution is one. We chose $a = 0.7$, $R_0^{ref} = 10$ nm, and $R_0^{max} = 100$ nm and we compute the evolution of the pressure, energy, and void fraction of a system in mechanical equilibrium.

Figure 4 depicts the system's Helmholtz free energy and the system's pressure versus void fraction. As for a single bubble, the system undergoes a tension stage along which the system's energy increases. When the largest bubble in the system reaches its critical radius (point A in Figure 4), the equilibrium pressure of the system, imposed by the Laplace equation at every bubble, starts to recover. In this case, although the largest bubble expands, the total volume of the system decreases due to the compression effect induced by the rest of bubbles that have not reached their critical radius. Thus, the void fraction and energy decrease down to point B. As the pressure is recovered, the gas volume increase induced by the largest bubble overcomes the compression experienced by the rest of the bubbles.

The curves obtained display a clear energy jump once the critical point A is reached. At this point, a differential increase on the system's volume (or void fraction) releases an important amount

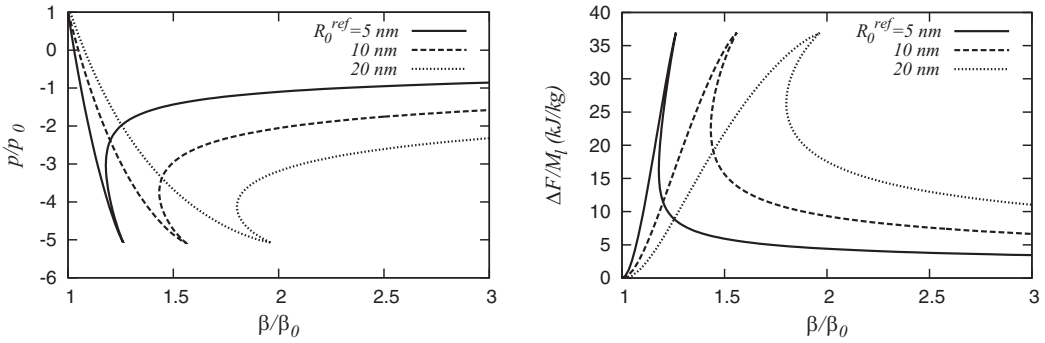

FIG. 5. Pressure (left) and Helmholtz free energy (right) of a polydisperse system versus void fraction for three bubble nuclei distributions centered at 5, 10, and 20 nm, respectively. The largest bubble present in the system is 100 nm for all cases. The maximum tension required to induce inception is controlled by the largest bubble and therefore it remains constant. The energy released at the inception point decreases as the averaged radius in the distribution increases.

of the elastic energy contained in the liquid. The energy jump can be obtained as a difference between the elastic energy of states A and C. The tension at which inception occurs increases as the largest bubble radius in the system decreases (R_0^{max}). That is, the energy stored at inception does not depend on the averaged properties of the bubble nuclei population present in the system, but on the size of the largest bubble contained in the system. However, the statistical properties of the bubble nuclei population do have an impact on the amount of energy released after inception. In this case, the initial bubble nuclei distribution and the ratio between the maximum radius and the averaged radius $R_0^{max}/\overline{R_0}$ control the amount of energy released. As shown in Figure 5, the larger this ratio, the stronger the potential energy jump.

It is convenient to define a critical value for the Helmholtz free energy as the liquid's elastic energy stored at point A ($\Delta F_c = \Delta F_A$), which is defined by the liquid's elastic energy at the Blake's radius of the largest bubble contained in the system. The corresponding void fraction at point A is then obtained by working out the equilibrium radius of all the bubbles contained in the system. This void fraction is used as a critical value (β_c) to define the relative deformation of the system using Eq. (6). The new normalized plot shown in Figure 6 resembles to standard diagrams of brittle

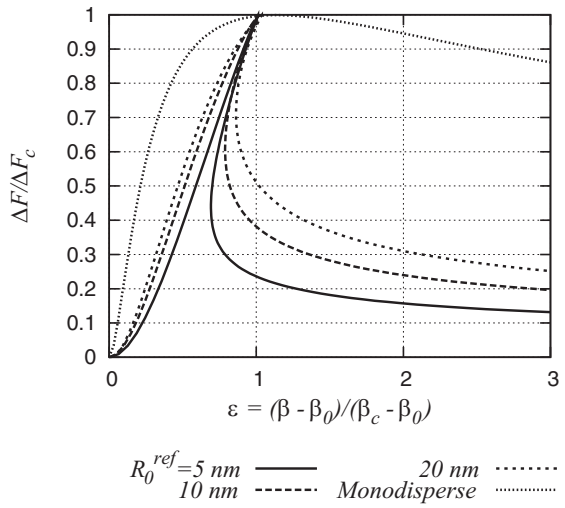

FIG. 6. Normalized diagrams for nondimensional tension vs. nondimensional displacement of the plots shown in Fig. 5. The shape of the curve is controlled by the bubble nuclei distribution function. For reference, a monodisperse case with bubbles with the largest radius has been included. The amount of elastic energy released by a polydisperse bubble cluster after the critical point increases for averaged radius.

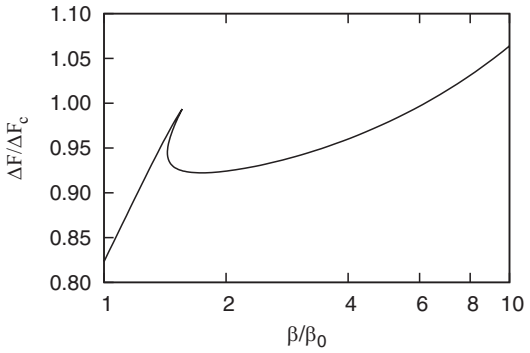

FIG. 7. Normalized total system energy versus void fraction for large initial gas concentrations ($\beta_0 \geq 10^{-3}$). The energy jump induced due to the polydispersity of the bubble distribution remains even at large void fractions.

fracture in solids. Beyond a critical deformation, which is small, fracture occurs and a phenomenon of snap back is observed depending on the internal structure of the material. In liquids, the relevance of this phenomenon is controlled by the polydispersity function of the bubble nuclei and therefore, we expect this function to play an important role on the energy released once the bubble inception point is reached.

It is also important to emphasize that the system's energy jump appears irrespective of the initial gas concentration (Figure 7). That is, although the initial amount of air still has a stabilizing effect in real applications, we will observe a sudden energy release once the cavitation threshold is reached due to polydispersity. This effect appears irrespective of the initial air concentration.

III. CONCLUSIONS

This work presents a novel analysis on the stability of multibubble systems. Using the derivative of the system's Helmholtz free energy with respect to the void fraction, we define the bubble inception conditions as the equilibrium states in which the bubble expansion is energetically favorable.

The current approach recovers the Blake threshold radius for the limit of a single bubble. For systems of multiple bubbles, the analysis reveals that the initial amount of air present in the system has a crucial impact on the stability properties of the system. For monodisperse systems, there is a critical concentration of gas above which the bubble expansion is no longer favorable. This value depends on the initial bubble radius and surface tension.

In addition, this analysis also reveals the importance of polydispersity in the process of sudden bubble expansion. The presence of bubbles of different sizes controls the amount of the liquid's elastic energy released after inception occurs. This effect turns out to occur irrespective of the initial amount of air.

[1] M. Blander and J. L. Katz, "Bubble nucleation in liquids," AIChE J. **21**(5), 833–848 (1975).
[2] M. J. Uline and D. S. Corti, "Activated instability of homogeneous bubble nucleation and growth," Phys. Rev. Lett. **99**(7), 076102 (2007).
[3] V. K. Shen and P. G. Debenedetti, "A kinetic theory of homogeneous bubble nucleation," J. Chem. Phys. **118**, 768 (2003).
[4] R. E. Apfel, "A novel technique for measuring the strength of liquids," J. Acoust. Soc. Am. **49**, 145 (1971).
[5] Q. Zheng, D. J. Durben, G. H. Wolf, and C. A. Angell, "Liquids at large negative pressures: Water at the homogeneous nucleation limit," Science **254**(5033), 829 (1991).
[6] X. H. Zhang, N. Maeda, and V. S. J. Craig, "Physical properties of nanobubbles on hydrophobic surfaces in water and aqueous solutions," Langmuir **22**(11), 5025–5035 (2006).
[7] W. A. Ducker, "Contact angle and stability of interfacial nanobubbles," Langmuir **25**(16), 8907–8910 (2009).
[8] A. P. Keller, "Investigations concerning scale effects of the inception of cavitation," in *Proceedings of the Institute of Mechanical Engineering Conference on Cavitation*, 1974.
[9] B. M. Borkent, S. M. Dammer, H. Schönherr, G. J. Vancso, and D. Lohse, "Superstability of surface nanobubbles," Phys. Rev. Lett. **98**(20), 204502 (2007).
[10] S. Witharana, B. Phillips, S. Strobel, H. D. Kim, T. McKrell, J.-B. Chang, J. Buongiorno, K. K. Berggren, L. Chen, and Y. Ding, "Bubble nucleation on nano- to micro-size cavities and posts: An experimental validation of classical theory," J. Appl. Phys. **112**, 064904 (2012).

[11] B. M. Borkent, M. Arora, and C. D. Ohl, "Reproducible cavitation activity in water-particle suspensions," J. Acoust. Soc. Am. **121**, 1406 (2007).
[12] A. J. Acosta and B. R. Parkin, "Cavitation inception: A selective review," J. Ship Res. **19**(4), 193–205 (1975).
[13] E. P. Rood, "Mechanisms of cavitation inception-review," ASME - J. Fluid Eng. **113**, 163–175 (1991).
[14] C. Brennen, *Cavitation and Bubble Dynamics* (Oxford University Press, New York, 1995), p. 254.
[15] A. A. Atchley and A. Prosperetti, "The crevice model of bubble nucleation," J. Acoust. Soc. Am. **86**, 1065 (1989).
[16] G. E. Reisman, M. E. Duttweiler, and C. E. Brennen, "Effect of air injection on the cloud cavitation of a hydrofoil," in *Proceedings of the ASME Fluid Engineering Division Summer Meeting*, Vancouver, June 1997.
[17] G. E. Reisman, Y. C. Wang, and C. E. Brennen, "Observations of shock waves in cloud cavitation," J. Fluid Mech. **355**, 255 (1998).
[18] T. Naoe, H. Kogawa, M. Futakawa, and M. Ida, "Mitigation technologies for damage induced by pressure waves in high-power mercury spallation neutron sources (III): Consideration of the effect of microbubbles on pressure wave propagation through a water test," J. Nucl. Sci. Technol. **48**, 865–872 (2011).
[19] F. G. Blake, Jr., "Onset of cavitation in liquids," Ph.D. thesis, Harvard University, 1949 (Source: American Doctoral Dissertations, Source code: W1949, 1949, p. 0049).
[20] E. A. Neppiras and B. E. Noltingk, "Cavitation produced by ultrasonics: Theoretical conditions for the onset of cavitation," Proc. Phys. Soc. B **64**(12), 1032 (1951).
[21] M. Ida, T. Naoe, and M. Futakawa, "Suppression of cavitation inception by gas bubble injection: A numerical study focusing on bubble-bubble interaction," Phys. Rev. E **76**, 046309 (2007).
[22] D. Fuster and T. Colonius, "Modeling bubble clusters in compressible liquids," J. Fluid Mech. **688**, 253–289 (2011).
[23] L. D. Landau and E. M. Lifshitz, *Fluid Mechanics* (Pergamon Press, Oxford, 1987).